

# Characterization of the acid–alkaline transition in the individual subunits of human adult and foetal methaemoglobins

Received April 14, 2010; accepted May 20, 2010; published online June 2, 2010

Tomokazu Shibata<sup>1</sup>, Satoshi Nagao<sup>1,\*</sup>,  
Hulin Tai<sup>1</sup>, Shigenori Nagatomo<sup>1</sup>,  
Hiromi Hamada<sup>2</sup>, Hiroyuki Yoshikawa<sup>2</sup>,  
Akihiro Suzuki<sup>3</sup> and Yasuhiko Yamamoto<sup>1,†</sup>

<sup>1</sup>Department of Chemistry, University of Tsukuba, Tsukuba 305-8571, <sup>2</sup>Institute of Clinical Medicine, University of Tsukuba, Tsukuba 305-8575 and <sup>3</sup>Department of Materials Engineering, Nagaoka College of Technology, Nagaoka 940-8532, Japan

\*Present address: Satoshi Nagao, Graduate School of Materials Science, Nara Institute of Science and Technology (NAIST), Nara 630-0192, Japan

†Yasuhiko Yamamoto, Department of Chemistry, University of Tsukuba, Tsukuba 305-8571, Japan. Tel: +81 29 853 6521, Fax: +81 29 853 6521, Email: yamamoto@chem.tsukuba.ac.jp

**Human adult haemoglobin (Hb A), a tetrameric oxygen transfer haemoprotein, has been recognized as an excellent model for investigating the structure–function relationships in allosteric proteins, and has been characterized exhaustively from both experimental and theoretical aspects. Despite the detailed structural and spectroscopic information available for the protein, functional properties have not been as fully elucidated as expected, and hence have remained unexplored. A major drawback for the functional characterization of Hb A is the lack of experimental techniques which enable quantitative characterization of functional properties of the individual subunits of the intact protein. In this study, we have developed techniques for determining the equilibrium constant of the acid–alkaline transition, usually represented as the ‘ $pK_a$ ’ value, in the individual subunits of the met-forms of Hb A (metHb A) and human foetal haemoglobin (metHb F). The  $pK_a$  values of the individual subunits of metHb A and metHb F have been shown to constitute novel and highly sensitive probes for characterizing the effects of structural changes of not only the interfaces between the subunits within the protein, but also the contact between haem and the protein in the haem pocket. In addition, haem replacement studies of the proteins revealed that the contact between the haem peripheral vinyl side chain and the protein in the haem pocket is important for maintaining the non-equivalence in the haem environment between the subunits of Hb A and Hb F, which could be relevant to the cooperative ligand binding of the proteins.**

**Keywords:** acid–alkaline transition/<sup>19</sup>F NMR/haemoglobin/myoglobin/thermodynamics.

**Abbreviations:** 7-PF, 13,17-bis(2-carboxylatoethyl)-3,8-diethyl-2,12,18-trimethyl-7-trifluoromethylporphyrinatoiron; Bis-Tris, Bis(2-hydroxyethyl)

iminotris(hydroxymethyl)methane; DFT, density functional theory; Hb A, human adult haemoglobin; Hb F, human foetal haemoglobin; Mb, myoglobin; mesohaem, 13,17-bis(2-carboxylatoethyl)-3,8-diethyl-2,7,12,18-tetramethylporphyrinatoiron; meso, mesohaem; metHb A, met-form of human adult haemoglobin; metHb F, met-form of human foetal haemoglobin; protohaem, Fe-protoporphyrin IX complex; TFA, trifluoroacetic acid.

Human adult haemoglobin (Hb A), a multimeric oxygen transport haemoprotein, is the best, albeit incompletely, understood allosteric protein in terms of its structure and function (1). Hb A has served as an excellent model for investigating the structure–function relationships in allosteric proteins. Hb A is a tetrameric protein consisting of two  $\alpha$  subunits of 141 amino acid residues and two  $\beta$  subunits of 146 residues, respectively (2). The  $\alpha$  and  $\beta$  subunits each contain one haem [Fe-protoporphyrin IX complex (protohaem) (Fig. 1A)] as a prosthetic group, to which oxygen molecule binds. The structures of the  $\alpha$  and  $\beta$  subunits are quite similar to each other and also to that of myoglobin (Mb), a monomeric oxygen storage haemoprotein, even though the sequence homology among them is only  $\sim 18\%$  (3).

In general, the functional properties of such proteins are characterized spectrophotometrically (4), since haem exhibits a characteristic absorption spectrum which sharply reflects changes in the haem Fe coordination state (5). Despite the high sensitivity of absorption spectra to the local haem environment, however, the line widths of the absorption spectra are too large to differentiate the haem environments of the individual subunits of Hb A.

There have been a number of studies attempting to characterize the functional properties of the individual subunits of Hb A, most of which have utilized artificial proteins, in which one of the subunits is chemically modified, *e.g.* metal ion substitution (6–16), to ruin its function in order to selectively evaluate the properties of the other intact subunit. Nevertheless questions must remain about the utilization of such chemically-modified proteins to isolate the functional properties of one of the subunits because of the presence of indirect effects of the modification. Hence, the development of techniques which enable quantitative characterization of the functional properties of the individual subunits of intact Hb A has been highly demanded, because

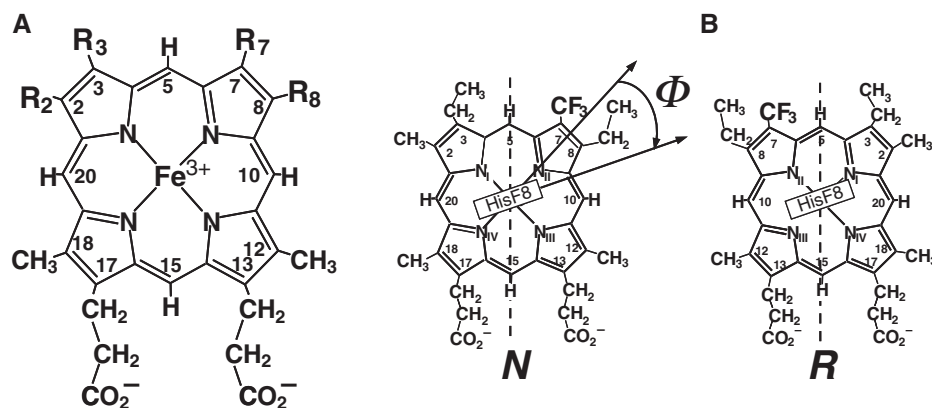
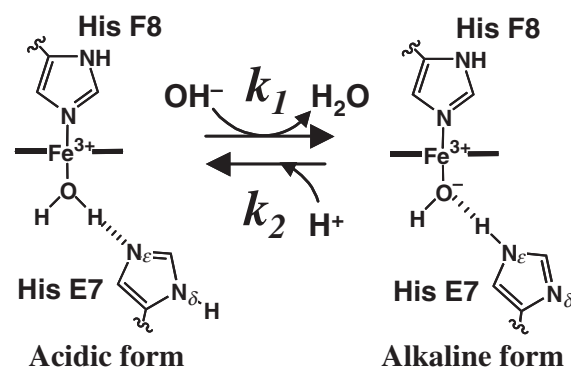


**Fig. 1** Molecular structure of haem and orientation of haem relative to His F8. (A) The structures and numbering system for protohaem ( $R_2 = \text{CH}_3$ ,  $R_3 = R_8 = \text{CH}=\text{CH}_2$ ,  $R_7 = \text{CH}_3$ ), mesohaem ( $R_2 = R_7 = \text{CH}_3$ ,  $R_3 = R_8 = \text{C}_2\text{H}_5$ ) and 7-PF ( $R_2 = \text{CH}_3$ ,  $R_3 = R_8 = \text{C}_2\text{H}_5$ ,  $R_7 = \text{CF}_3$ ). (B) Two possible orientations of the haem relative to His F8, *N* and *R* forms. The  $\Phi$  value represents the angle between the projection of the axial His imidazole onto the haem plane and the  $\text{N}_{11}\text{-Fe-N}_{1V}$  axis.

they are expected to provide experimental data which directly reflect the subunit interactions responsible for the cooperative oxygen binding of Hb A, and hence important clues for elucidating the structure–function relationship in the protein. In fact, taking advantage of subunit-specific isotope labelling techniques applicable to Hb A (17–20), the preparation of the so-called valency hybrid Hb A possessing ferrohaem in one subunit and ferrihaem in the other, (15, 21) or the high sensitivity of paramagnetic NMR in distinguishing the individual subunits of the protein (22, 23), some attempts have been successful in the characterization of the functional properties of the individual subunits of the intact protein.

In this study, we develop techniques which allow characterization of ‘the acid–alkaline transition’ in the subunits of the met form of Hb A (metHb A). The haem active sites in metHb A and the met forms of Mb (metMb) exhibit characteristic pH-dependent structure changes collectively known as the acid–alkaline transition (5). The subunits of metHb A as well as metMb possessing highly conserved distal His E7 [E7 represents an alphanumeric code referring to the positions of amino acid residues in the helices and turns of Hb and Mb, E7 represents the seventh residue in the E helix (see the amino acid sequences of the proteins in Supplementary Material SM1)] have H<sub>2</sub>O and OH<sup>-</sup> as coordinated external ligands under low and high pH conditions, respectively (5, 24–31). As illustrated in Scheme 1 (32), the acid–alkaline transition in the proteins comprises three distinct reactions, *i.e.* interconversion of the coordinated ligand between H<sub>2</sub>O and OH<sup>-</sup>, tautomerism of the His E7 imidazole and deprotonation/protonation of His E7 N<sub>δ</sub>H (31). Furthermore, since the transition is associated with the deprotonation/protonation process, its equilibrium constant is usually represented as the ‘p*K*<sub>a</sub>’ value in analogy with the ionization equilibrium of an acid. The p*K*<sub>a</sub> value has been shown to remarkably vary with the protein, ranging from 7.2 to 10 (5, 24–31), indicating that the acid–alkaline transition in the protein sharply reflects characteristics of the structural features of the haem active site (24–31). In addition,



**Scheme 1** The acid–alkaline transition in metMb, and the subunits of metHb A and metHb F.

we have recently demonstrated both experimentally and theoretically that the p*K*<sub>a</sub> value in Mb is highly sensitive to electronic nature of haem peripheral side chains (33). Furthermore, the sensitivity of the p*K*<sub>a</sub> value to the haem environment has also been confirmed by the observation that the value is affected by the well-documented haem orientational disorder (34) resulting from the incorporation of haem into the apoprotein in two orientations differing by 180° rotation about the 5,10-*meso* axis (Fig. 1B) (31).

One of our techniques is based on quantitative fitting of the pH-dependent change in the absorption spectra of the protein to the sum of two Henderson–Hasselbalch equations, with the assumption of non-equivalent p*K*<sub>a</sub> values for the constituent  $\alpha$  and  $\beta$  subunits of metHb A. The other two techniques take advantage of the preparation of the valency hybrid metHb A (35), in which ferrihaem is accommodated in one subunit, *i.e.* either the  $\alpha$  or  $\beta$  subunit, and ferrohaem in the other, and <sup>19</sup>F NMR in combination with fluorinated haem. For the former technique, the acid–alkaline transition in only the subunit possessing ferrihaem is reflected in the pH-profile of the absorption spectra of the prepared hybrid protein. For the latter one, as reported previously (36–41), NMR signals arising from fluorine atoms introduced into the haem as peripheral side chain(s) are extremely sensitive

to the haem electronic structure. In particular, fluorinated haems possessing  $\text{CF}_3$  group(s) such as 13,17-bis(2-carboxylatoethyl)-3,8-diethyl-2,12,18-trimethyl-7-trifluoro-methyl-porphyrinatoiron (III) (36) (7-PF; Fig. 1A) exhibit relatively narrow  $^{19}\text{F}$  NMR signals, even though the haem is incorporated into an apoprotein with a large molecular weight, mainly because of its relatively small chemical shift anisotropy, which largely contributes to the  $^{19}\text{F}$  relaxation (42, 43). In addition, the Curie spin relaxation mechanism effect (44, 45) is also expected to be small for the  $^{19}\text{F}$  relaxation of  $\text{CF}_3$  due to its rapid rotation around the  $C_3$  axis. These three techniques have been applied to determine the  $\text{p}K_a$  values of the subunits of not only metHb A, but also the met form of human foetal haemoglobin (46) (metHb F) composed of two  $\alpha$  subunits and two  $\gamma$  subunits of 146 amino acid residues, respectively, in order to characterize the haem active sites in the individual subunits of the proteins. Furthermore, the  $\text{p}K_a$  values of the  $\alpha$ ,  $\beta$  and  $\gamma$  subunits of metHb A and metHb F were compared with those of the corresponding subunits in their isolated states to gain an insight into the effect of the hetero-tetramer assembly on the haem environments of the subunits. Considering that the isolated  $\alpha$  and  $\beta$  subunits, which exist as a dimer (47) and a tetramer (47–49), respectively, do not exhibit cooperative ligand binding at all, the non-equivalence in the haem environment between the constituent subunits within a tetrameric Hb, together with the molecular mechanisms which allow transmission of structural changes among the haem active sites of the subunits, is thought to be indispensable for the cooperativity of Hb. The high sensitivity of the  $\text{p}K_a$  value to the nature of the haem active site is expected to permit detailed characterization of the haem environments of the subunits of metHb A and metHb F. Finally, the  $\text{p}K_a$  values of Hb A and Hb F reconstituted with mesohaem (Fig. 1A) and 7-PF were determined and compared with each other and with those of native Hbs in order to determine the effect of the haem-protein interaction on the haem environments of the constituent subunits.

We report herein the development of techniques for determination of the  $\text{p}K_a$  values of the subunits of metHb A and metHb F. The subunit interactions in the proteins was clearly manifested in the  $\text{p}K_a$  values of metHb A, metHb F, the isolated subunits and valency hybrid proteins. In addition, since the  $\text{p}K_a$  value has been shown to be highly affected by the electronic nature of the haem peripheral side chains, we have analysed the relationship between the  $\text{p}K_a$  value and the conformation of the haem vinyl side chains through the analysis of well-known Mulliken charge analysis using density functional theory (DFT) calculations. The calculations suggested that the  $\text{p}K_a$  value is largely affected through the electronic interaction between the porphyrin and vinyl  $\pi$ -systems. Finally, comparison of the  $\text{p}K_a$  values between metHb A and the protein reconstituted with mesohaem or 7-PF revealed that the contact between the haem peripheral vinyl side chains and the protein is important for maintaining the non-equivalence in the haem environment between the  $\alpha$  and  $\beta$  subunits of the protein.

## Materials and Methods

### Protein Samples

Hb A was prepared from blood obtained from the Medical Center of the University of Tsukuba using the reported procedure (50). Hb F was isolated and purified in the carbonmonoxy (CO) form from the blood withdrawn from the umbilical cord of a patient, who agreed to the donation, in the Medical Center according to the method previously described (51).  $\alpha$ ,  $\beta$  and  $\gamma$  subunits were isolated from Hb A and Hb F according to the method previously described (52, 53). The quality of each Hb subunit was confirmed with a Mass Spectrometer, QStar/Pulsar *i* (Applied Biosystems). Valency hybrid  $\alpha$ -metHb A ( $\alpha$ -metHb F) possessing ferrihaem in the  $\alpha$  subunit and ferrohaem in the  $\beta$  ( $\gamma$ ) one was prepared from metHb A (metHb F) using the reported procedure (54). Valency hybrid  $\beta$ -metHb A ( $\gamma$ -metHb F) possessing ferrohaem in the  $\alpha$  subunit and ferrihaem in the  $\beta$  ( $\gamma$ ) one was prepared through reassembly of the isolated  $\alpha$ ,  $\beta$  and  $\gamma$  subunits according to the method previously described (55). In the valency hybrid proteins prepared, CO is coordinated as an external ligand to haem Fe of ferrohaem. The quality of each hybrid protein was confirmed by analysis of  $^1\text{H}$  NMR spectra of their azide adducts (Fig. 2). MetHb A and metHb F were prepared from the CO forms of the proteins under a stream of  $\text{O}_2$  gas with strong illumination in the presence of a 5-fold molar excess of potassium ferricyanide (Wako Chemical Co.). The protein was separated from the residual chemicals using a Sephadex G-50 (Sigma Chemical Co.) column equilibrated with 50 mM Bis-Tris (Sigma Chemical Co.), pH 6.5. 7-PF was synthesized as previously described (31). Protohaem was purchased from Sigma Chemical Co. Mesohaem (Fig. 1A) was prepared from mesoporphyrin IX dimethyl ester purchased from Aldrich Chemical Co. Sperm whale Mb was purchased as a lyophilized powder from Biozyme and used without further purification. The apoprotein of Hb was prepared at  $4^\circ\text{C}$  according to the procedure of Teale (56), and reconstitution of the apoprotein with haem was carried out by the standard procedure (50). The reconstituted Hb A and Hb F were concentrated to  $\sim 1$  mM in an ultra-filtration cell (Amicon). The pH of each sample was measured with a Horiba F-22 pH meter equipped with a Horiba type 6069-10c electrode. The pH of the sample was adjusted using 0.2 M NaOH or HCl.

### UV–vis absorption and NMR spectroscopies

UV–vis absorption spectra were recorded at  $25^\circ\text{C}$  with a Beckman DU 640 spectrophotometer and a protein concentration of  $10\ \mu\text{M}$  in 20 mM phosphate buffer.  $^1\text{H}$  NMR and  $^{19}\text{F}$  NMR spectra were recorded on a Bruker AVANCE-400 spectrometer operating at the  $^1\text{H}$  and  $^{19}\text{F}$  frequencies of 400 and 376 MHz, respectively. Typical  $^1\text{H}$  and  $^{19}\text{F}$  NMR spectra consisted of  $\sim 20$  k transients with a 100 kHz spectral width and 16 k data points. The signal-to-noise ratio of each spectrum was improved by apodization, which introduced 20–100 Hz line broadening. The chemical shifts of  $^1\text{H}$  and  $^{19}\text{F}$  NMR spectra are given in ppm downfield from the residual  $^1\text{H}_2\text{O}$ , as an internal reference, and from trifluoroacetic acid, as an external reference, respectively.

### DFT calculation

Evaluation of the electron density of the haem Fe atom ( $\rho_{\text{Fe}}$ ) value was carried out by Mulliken charge analysis through the DFT calculations carried out using the Gaussian 03 programme package (57). Restricted spin orbital approach involving the B3LYP method, together with electron basis sets of Pople's 6-31G(d), was employed. For simplification, the calculations were performed for the 3,8-divinylporphyrinatoiron(II) complex as a model for the protohaem (Supplementary Material SM2B). Geometry optimization of the model compounds was carried out in the gas phase, with a fixed vinyl group conformation possessing the dihedral angles  $\text{C}_2\text{—C}_3\text{—C}_\alpha\text{—C}_\beta$  ( $\Psi_{3\text{-vinyl}}$ ) and  $\text{C}_7\text{—C}_8\text{—C}_\alpha\text{—C}_\beta$  ( $\Psi_{8\text{-vinyl}}$ ) of  $0^\circ$  (Fig. 3), *i.e.* all vinyl group atoms were in the porphyrin plane (Supplementary Material SM2B), and then single point calculations of the model compound were carried out with changing the  $\Psi_{3\text{-vinyl}}$  and  $\Psi_{8\text{-vinyl}}$  values by  $5^\circ$  steps between  $0^\circ$  and  $90^\circ$  in order to analyse the relationship between the  $\rho_{\text{Fe}}$  value and dihedral angle (Fig. 3). The oxidation, spin and coordination states of the haem Fe atoms of the model compound were assumed to be Fe(II),  $S=0$ , and a six-coordinated structure with CO ligands, respectively (Supplementary Material SM2B).

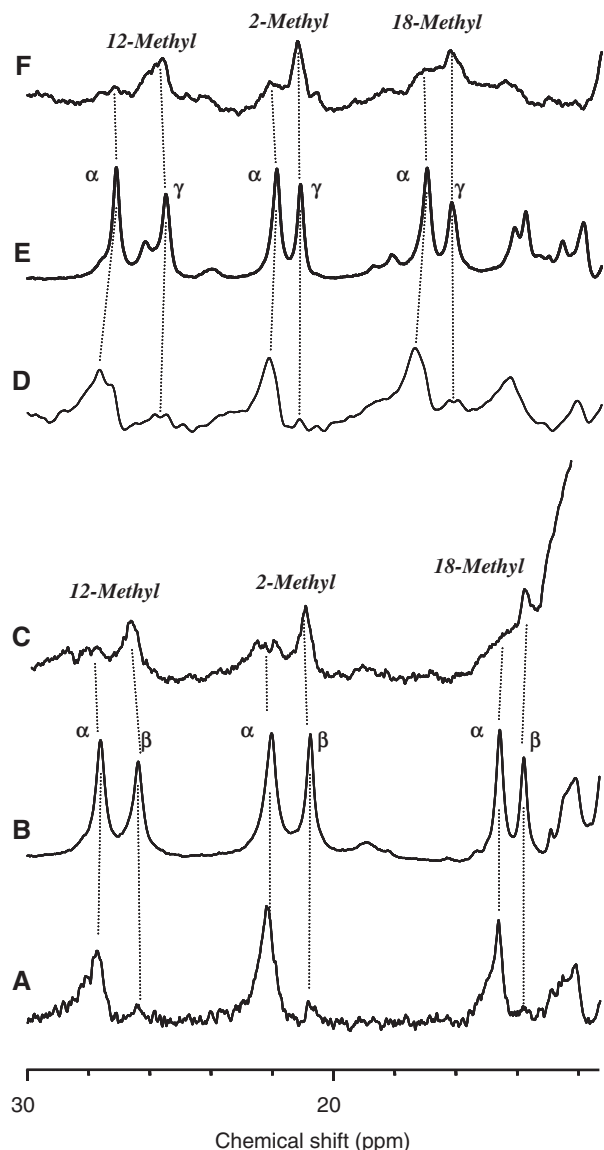


**Fig. 2** 400 MHz  $^1\text{H}$  NMR spectra of met-azido Hbs.  $^1\text{H}$  NMR spectra (400 MHz) of the met-azido forms of valency hybrid  $\alpha$ -metHb A (A), metHb A (B), valency hybrid  $\beta$ -metHb A (C), valency hybrid  $\alpha$ -metHb F (D), metHb F (E) and valency hybrid  $\gamma$ -metHb F (F) at pH 7.0. (A–C) and (D–F) were recorded at 25 and 45°C, respectively. The corresponding haem methyl proton signals are connected by dotted lines. In the spectra of valency hybrid Hbs, signals due to the subunit possessing a ferrihaem with a coordinated CO are not observed in the indicated chemical shift region, because of the absence of unpaired electrons.

## Results

### Determination of the $pK_a$ values of the constituent subunits of metHb A and metHb F

The pH dependence of the absorption spectra of metHb A at 25°C and plots of 575-nm absorption against pH are presented in Fig. 4A and B, respectively. Quantitative fitting of the plots to the Henderson–Hasselbalch equation yielded an ‘apparent  $pK_a$  value’ of  $7.90 \pm 0.05$  (Supplementary Material SM3). Careful scrutiny revealed that the fitting with a single Henderson–Hasselbalch equation resulted in systematic errors as to the observed and theoretical values,

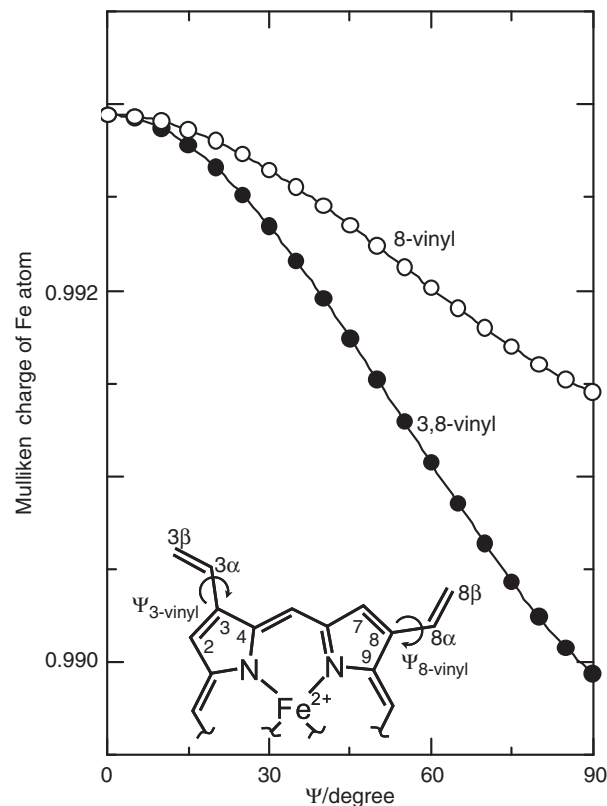


**Fig. 3** Plots of calculated Mulliken charges of haem Fe atom against the  $\Psi_{8\text{-vinyl}}$  value, with a fixed  $3\text{-vinyl}$  side chain conformation at  $\Psi_{3\text{-vinyl}} = 0^\circ$ , (open circle) and the  $\Psi_{3\text{-vinyl}}$  and  $\Psi_{8\text{-vinyl}}$  values, which changed simultaneously by  $5^\circ$  steps (filled circle). The definition of the dihedral angles  $\text{C}2\text{--C}3\text{--C}\alpha\text{--C}\beta$  ( $\Psi_{3\text{-vinyl}}$ ) and  $\text{C}7\text{--C}8\text{--C}\alpha\text{--C}\beta$  ( $\Psi_{8\text{-vinyl}}$ ) is illustrated in the inset; *s-cis* vinyl side chain conformation with all vinyl group atoms being in the porphyrin plane is defined to be  $0^\circ$ .

*i.e.* the observed values were larger and smaller than the theoretical ones in lower and higher pH regions relative to the apparent  $pK_a$  value, respectively (Supplementary Material SM3). With the assumption of non-equivalence in the  $pK_a$  value between the  $\alpha$  and  $\beta$  subunits of metHb A, the plots were significantly better fitted with the sum of two Henderson–Hasselbalch equations, yielding  $pK_a$  values of  $7.48 \pm 0.05$  and  $8.32 \pm 0.05$  (Supplementary Material SM2).

In order to assign the obtained  $pK_a$  values to the subunits of metHb A, the  $pK_a$  value of valency hybrid  $\alpha$ -metHb A ( $\beta$ -metHb A) possessing ferrihaem in the  $\alpha$  ( $\beta$ ) subunit and ferrihaem in the  $\beta$  ( $\alpha$ ) one was similarly determined. In these hybrid proteins, the acid–alkaline transition in only the subunit possessing ferrihaem is reflected in the pH-profile of the absorption spectra. The  $pK_a$  values of  $8.27 \pm 0.10$  and  $7.61 \pm 0.10$  were obtained for  $\alpha$ -metHb A and  $\beta$ -metHb A, respectively (Supplementary Material SM4). These results unequivocally indicated that the  $pK_a$  values of  $8.32 \pm 0.05$  and  $7.48 \pm 0.05$ , obtained on fitting of the metHb A plots using the sum of two Henderson–Hasselbalch equations, are due to the  $\alpha$  and  $\beta$  subunits of metHb A, respectively.

Similarly, on fitting of the pH-dependent 575-nm absorption of metHb F with the sum of two

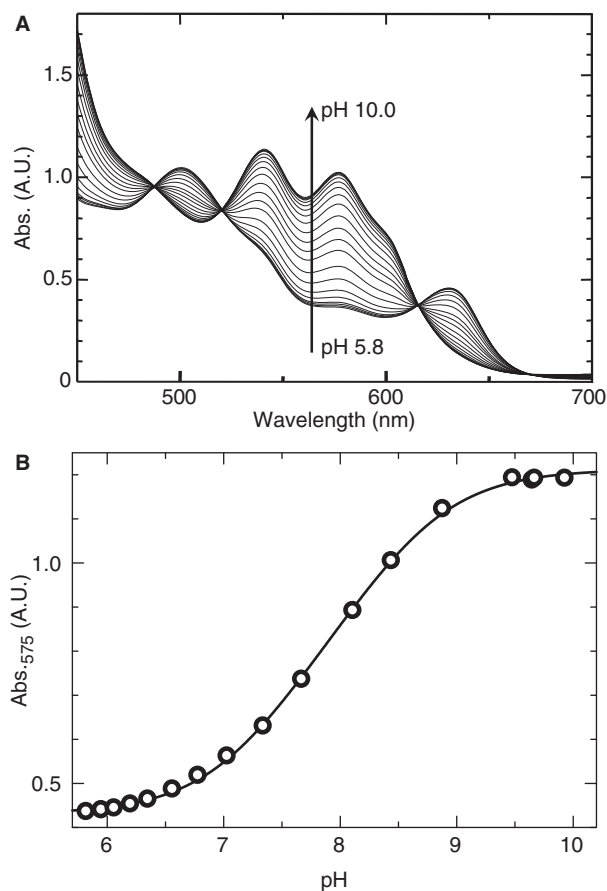


**Fig. 4** Analysis of the acid-alkaline transition of metHb A. pH-dependent optical spectra, 450–700 nm, of metHb A (A), and  $pK_a$  values of  $7.48 \pm 0.05$  and  $8.32 \pm 0.05$  obtained from plots of absorbance at 575 nm against pH (B).

Henderson–Hasselbalch equations, the  $pK_a$  values of  $7.76 \pm 0.05$  and  $8.48 \pm 0.05$  were obtained (Supplementary Material SM5). Considering the  $pK_a$  values of  $8.27 \pm 0.1$  and  $7.89 \pm 0.10$  obtained for valency hybrid  $\alpha$ -metHb F and  $\gamma$ -metHb F, respectively (Supplementary Material SM6), the  $8.48 \pm 0.05$  and  $7.76 \pm 0.05$  yielded for metHb F could be due to the  $pK_a$  values of the  $\alpha$  and  $\gamma$  subunits of metHb F, respectively. The appreciable differences in the  $pK_a$  values between the corresponding subunits of metHb A (or metHb F) and valency hybrid metHb A (or metHb F) indicated that the structural properties of one subunit in Hb A (or Hb F) are affected by the haem Fe oxidation and coordination states of the other.

#### Determination of the $pK_a$ values of the isolated $\alpha$ , $\beta$ and $\gamma$ subunits

We next similarly determined the  $pK_a$  values of the isolated  $\alpha$ ,  $\beta$  and  $\gamma$  subunits through analysis of the pH dependence of the optical spectra.  $pK_a$  values of  $8.17 \pm 0.05$ ,  $7.75 \pm 0.05$  and  $8.26 \pm 0.05$  were obtained for the isolated  $\alpha$ ,  $\beta$  and  $\gamma$  subunits, respectively (Fig. 5 and Table I), which were different from those of the corresponding subunits of metHb A and metHb F in Table I, indicating that the  $pK_a$  values of the subunits

were significantly affected by the hetero-tetramer assembly.

#### Absorption spectra of Hb A, Hb F and their constituent subunits

We measured the absorption spectra of the CO forms of Hb A, Hb F and their constituent subunits, and the absorption maxima ( $\lambda_{max}$ ) are summarized in Table II. The  $\lambda_{max}$  values observed for Hb A and isolated  $\alpha$  and  $\beta$  subunits were similar to those previously reported (58). Assuming that the  $\lambda_{max}$  values of Hb A and Hb F represent those of the constituent subunits, comparison of the  $\lambda_{max}$  values among the Hbs and isolated subunits indicated that the hetero-tetramer assembly results in bathochromic and hypochromic shifts of the absorption of  $\alpha$  subunit, and  $\beta$  and  $\gamma$  subunits, respectively. Since the Soret absorption has been shown to exhibit bathochromic shift with increasing the polarity of solvent (59), the present results supported that the haem environments of the  $\alpha$  subunit, and the  $\beta$  and  $\gamma$  subunits become more polar and less polar upon the hetero-tetramer assembly.

#### Determination of the $pK_a$ value of metHb A reconstituted with mesohaem

We also determined the  $pK_a$  value of metHb A reconstituted with mesohaem [metHb A(Meso)]. Fitting of the pH-dependent 575-nm absorption to the Henderson–Hasselbalch equation yielded the apparent  $pK_a$  value of  $8.50 \pm 0.05$ , and, in contrast to the case of native metHb A, the use of two Henderson–Hasselbalch equations for the fitting did not improve the agreement between the observed and theoretical values (Supplementary Material SM7). These results indicated that the  $pK_a$  values of both the  $\alpha$  and  $\beta$  subunits of metHb A(Meso) are  $\sim 8.5$ . Considering that the  $pK_a$  values for the  $\alpha$  and  $\beta$  subunits of native metHb A are  $8.32 \pm 0.05$  and  $7.48 \pm 0.05$ , respectively, the substitution of haem peripheral vinyl side chains by ethyl groups, as a result of the haem replacement, was found to reduce the non-equivalence of the  $pK_a$  values between the  $\alpha$  and  $\beta$  subunits of metHb A, and also to increase the  $pK_a$  values of the  $\alpha$  and  $\beta$  subunits by  $\sim 0.3$  and  $1.1$  pH units, respectively.

Similarly,  $8.50 \pm 0.05$  was determined for the  $pK_a$  value of metHb F reconstituted with mesohaem [metHb F(Meso)] (Supplementary Material SM7). Consequently, as in the case of Hb A, the replacement of protohaem by mesohaem resulted in the loss of the non-equivalence in the  $pK_a$  value between the subunits of metHb F, and increases in the  $pK_a$  values of the  $\alpha$  and  $\gamma$  subunits by  $\sim 1.0$  and  $0.7$  pH units, respectively.

#### Determination of the $pK_a$ values of the subunits of metHb A and metHb F reconstituted with 7-PF

$^{19}\text{F}$  NMR spectra of metHb A and metHb F reconstituted with 7-PF [metHb A(7-PF) and metHb F(7-PF), respectively] at  $25^\circ\text{C}$  and basic pH, together with that of metMb(7-PF) at pH 10.91, are shown in Fig. 6A. The line widths of the Hb signals, *i.e.* 600–800 Hz, were larger than those of the Mb ones, *i.e.*  $\sim 500$  Hz,

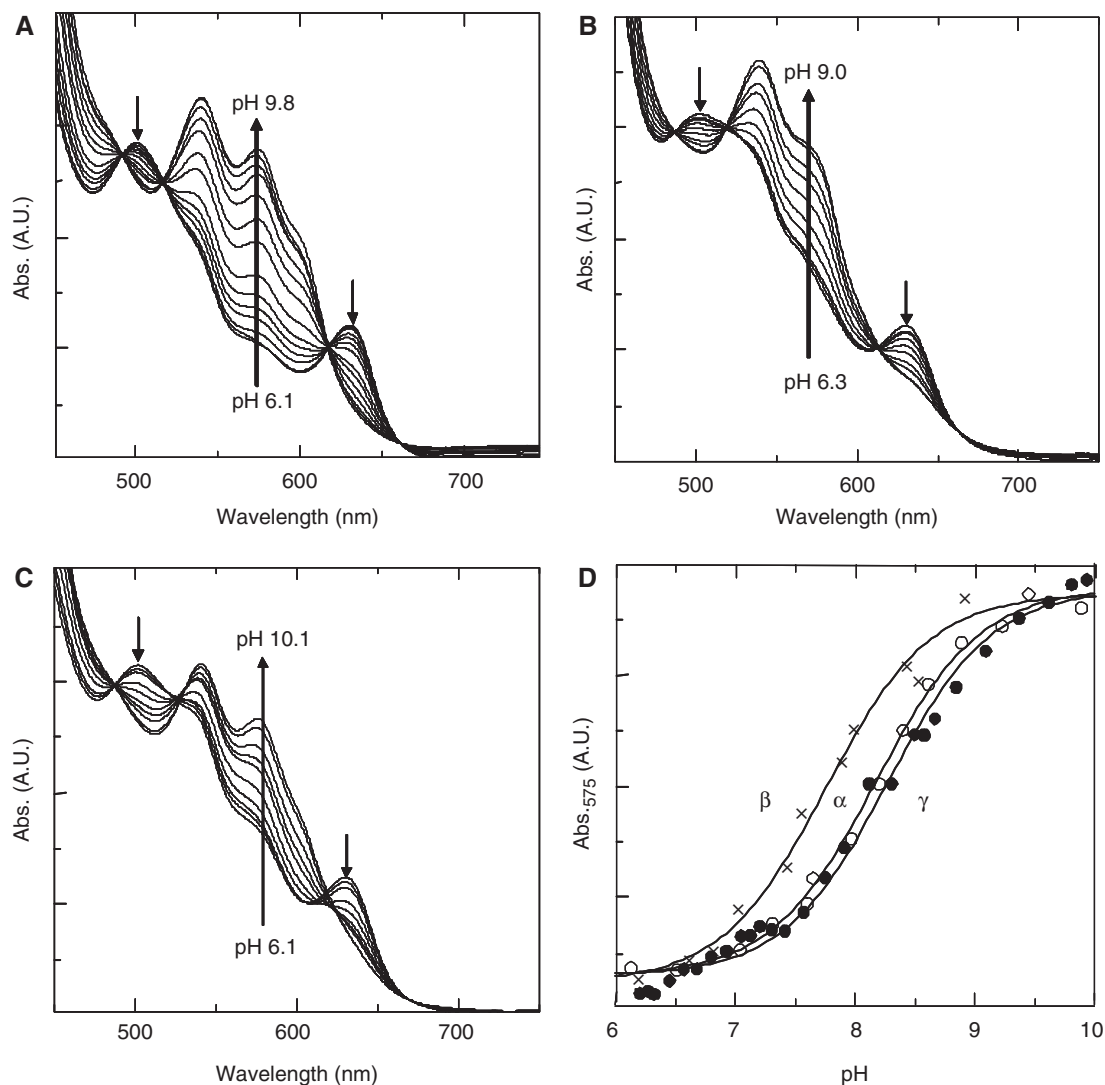


**Fig. 5** Analysis of the acid-alkaline transition of met-forms of isolated subunits. pH-dependent optical spectra, 450–750 nm, of the isolated  $\alpha$  subunit (A),  $\beta$  subunit (B) and  $\gamma$  subunit (C), and  $pK_a$  values of  $8.17 \pm 0.05$ ,  $7.75 \pm 0.05$  and  $8.26 \pm 0.05$  obtained from plots of 575 nm-absorbance for the isolated  $\alpha$ ,  $\beta$  and  $\gamma$  subunits, respectively (D).

**Table I.** The  $pK_a$  values of metHb A, metHb F, Hybrid Hbs and isolated subunit at 25°C.

	metHb A	metHb F	Hybrid Hb	Isolated subunit
$\alpha$	$8.32 \pm 0.05$	$8.48 \pm 0.05$	$8.27 \pm 0.10$	$8.17 \pm 0.05$
$\beta$	$7.48 \pm 0.05$	—	$7.61 \pm 0.10$	$7.75 \pm 0.05$
$\gamma$	—	$7.76 \pm 0.05$	$7.89 \pm 0.10$	$8.26 \pm 0.05$

possibly due to the difference in size between the proteins. Two signals due to the haem orientational disorder were observed in the spectrum of metMb(7-PF), the ratio being 1.0:2.2 for *N* form: *R* form at equilibrium (Fig. 6A) (31). On the other hand, in the spectra of metHb A(7-PF) and metHb F(7-PF), three signals, peaks  $a_i$ – $c_i$  ( $i = A$  or  $F$ ), were resolved. These signals could be assigned through analysis of their intensities, and spectral comparison between metHb A(7-PF) and metHb F(7-PF). First of all, the sum of the intensities of peaks  $a_i$  and  $b_i$  was almost the same as that of peak  $c_i$ , indicating that the former signals arise from one

**Table II.** The absorption maximum wavelength ( $\lambda_{max}$ ) of CO forms of Hb A, Hb F and their constituent subunit at pH 7.00 and 25°C.

	Soret (nm)		Visible (nm)	
	Hb A or Hb F	Isolated subunits	Hb A or Hb F	Isolated subunits
$\alpha$	419.5	418.5	537.0	538.5 <sup>a</sup>
$\beta$	419.5	420.0	568.0	568.5
			540.0	538.5
$\gamma$	419.5	420.8	569.5	568.5
			539.2	538.0
			569.4	568.5

<sup>a</sup>Taken from the value of Hb A. The value of Hb F is 538.0 nm.

subunit and hence the latter ones from the other. In addition, the shifts of peaks  $a_A$  and  $b_A$ , *i.e.* 71.2 and 63.0 ppm, respectively, are similar to those of peaks  $a_F$  and  $b_F$ , *i.e.* 71.0 and 62.9 ppm, respectively, suggesting that peaks  $a_i$  and  $b_i$  arise from the  $\alpha$  subunit, which is common to both Hb A and Hb F. Hence, peaks  $c_A$  and

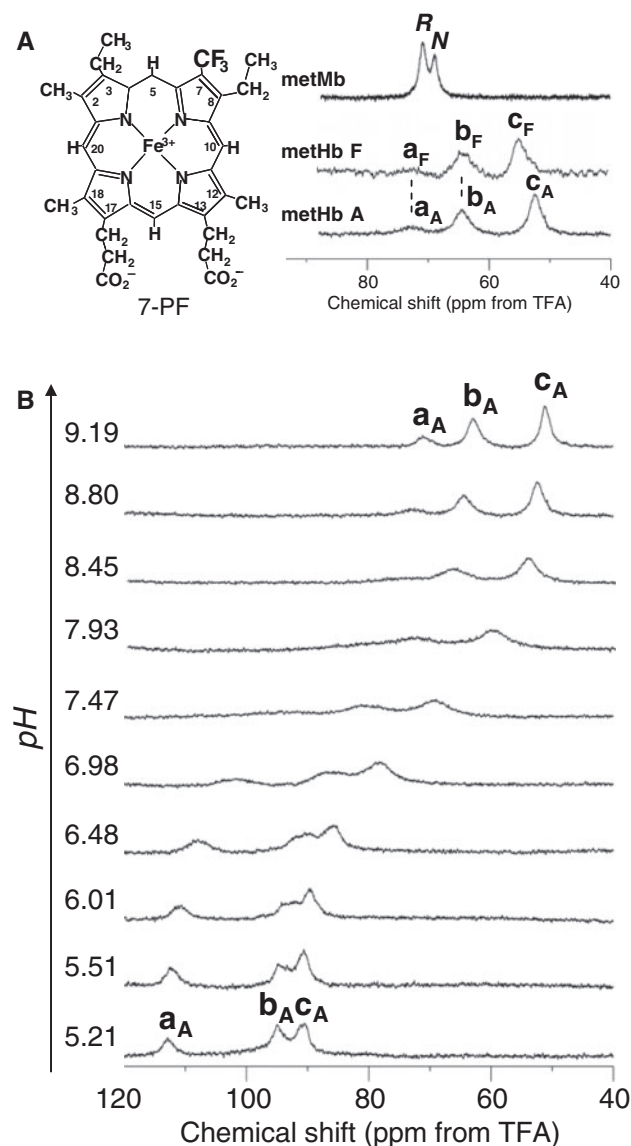


**Fig. 6** 470 MHz  $^{19}\text{F}$  NMR spectra of methHb A(7-PF). (A) 470 MHz  $^{19}\text{F}$  NMR spectra of methHb A(7-PF) at pH 9.0, methHb F(7-PF) at pH 9.0, and metMb(7-PF) at pH 10.91. Three peaks,  $a_i$ – $c_i$  ( $i = \text{A}$  or  $\text{F}$ ), were observed in the spectrum of each of methHb A(7-PF) and methHb F(7-PF). In the spectrum of methHb A(7-PF), peaks  $a_A$  and  $b_A$  are assigned to the  $N$  and  $R$  forms of the  $\alpha$  subunit, and  $c_A$  to either the  $N$  or  $R$  form of the  $\beta$  subunit (see text). Similarly, in the spectrum of methHb F(7-PF), peaks  $a_F$  and  $b_F$  are assigned to the  $N$  and  $R$  forms of the  $\alpha$  subunit, and  $c_F$  to either the  $N$  or  $R$  form of the  $\gamma$  subunit (see text). The assignments of two signals, due to the haem orientational disorder, in the spectrum of metMb(7-PF)<sup>14</sup> are indicated in the spectrum. Structure of 7-PF is also illustrated. (B) The spectra of methHb A(7-PF) at 25°C and the indicated pH values.

$c_F$  observed at 51.3 and 53.1 ppm, respectively, are assigned to the  $\beta$  and  $\gamma$  subunits of the proteins, respectively. Consequently, the shift differences between the two signals due to the haem orientational disorder were found to be larger for Hbs, *i.e.* 8.06 and 9.23 ppm for methHb A(7-PF) and methHb F(7-PF), respectively, than metMb(7-PF), *i.e.* 2.30 ppm. Furthermore, assuming that the  $R$  form dominates over the  $N$  one, as in the case of metMb(7-PF), peaks  $a_i$  and  $b_i$  are tentatively assigned to the  $N$  and  $R$  forms, respectively. Thus, peaks  $a_A$  and  $b_A$  could be

assigned to the  $N$  and  $R$  forms of the  $\alpha$  subunit of methHb A(7-PF), respectively [ $\alpha_{A(N)}$  and  $\alpha_{A(R)}$ , respectively], and  $a_F$  and  $b_F$  to the  $N$  and  $R$  forms of the  $\alpha$  subunit of methHb F(7-PF), respectively [ $\alpha_{F(N)}$  and  $\alpha_{F(R)}$ , respectively]. Analysis of the signal intensities revealed that the ratios for  $N$  form:  $R$  form for the  $\alpha$  subunits of methHb A(7-PF) and methHb F(7-PF) are  $\sim 1:3$ , and, on the other hand, the haem orientational disorder in both the  $\beta$  subunit of methHb A(7-PF) and the  $\gamma$  subunit of methHb F(7-PF) is negligible, if any.

With decreasing pH, the signals exhibited progressive downfield shifts of  $\sim 40$ – $50$  ppm. The acid–alkaline transition in the protein was manifested in the large pH-induced shift changes attributable to a change in the spin state between the acidic (essentially  $S = 5/2$ ) and alkaline (mainly  $S = 1/2$ ) forms (Fig. 6B). Quantitative fitting of their pH-dependent shifts to the Henderson–Hasselbach equation yielded  $\text{p}K_a$  values of  $7.55 \pm 0.05$ ,  $7.59 \pm 0.05$  and  $7.38 \pm 0.05$  for the  $N$  and  $R$  forms of the  $\alpha$  subunit, and the  $\beta$  subunit of methHb A(7-PF), respectively (Fig. 7). On the other hand, an optical study of methHb A(7-PF) yielded a  $\text{p}K_a$  value of  $7.52 \pm 0.05$  (see Supplementary Material SM8). Similarly,  $\text{p}K_a$  values of  $7.50 \pm 0.05$ ,  $7.60 \pm 0.05$  and  $7.61 \pm 0.05$  were obtained for the  $N$  and  $R$  forms of the  $\alpha$  subunit, and the  $\gamma$  subunit of methHb F(7-PF), respectively (Fig. 7). The obtained  $\text{p}K_a$  values are summarized in Table III.

#### DFT calculations

We have recently shown that the  $\text{p}K_a$  value is closely related to the  $\rho_{\text{Fe}}$  value which is determined by electronic nature of the haem peripheral side chains (33). Since the electronic effect of the haem vinyl side chains on the porphyrin  $\pi$ -system is thought to be affected by the vinyl side chain conformation, we have carried out DFT calculations using a model compound (see ‘Materials and Methods’ section, and Supplementary Material SM2 for details) in order to quantitatively assess the relationship between the  $\Psi_{3\text{-vinyl}}$  and  $\Psi_{8\text{-vinyl}}$  values and the  $\rho_{\text{Fe}}$  value. The  $\rho_{\text{Fe}}$  value was estimated on the basis of the Mulliken charge of the haem Fe atom. The obtained Mulliken charge decreased with increasing the  $\Psi_{3\text{-vinyl}}$  and  $\Psi_{8\text{-vinyl}}$  values from  $0^\circ$  to  $90^\circ$ , and the  $\Psi_{3\text{-vinyl}}$  and  $\Psi_{8\text{-vinyl}}$  values were found to alter the Mulliken charge in an additive manner (Fig. 3). Although the Mulliken charges were calculated for the ferrous model compounds, a similar relationship between the  $\rho_{\text{Fe}}$  value and the  $\Psi_{3\text{-vinyl}}$  and  $\Psi_{8\text{-vinyl}}$  values is also expected for the ferrihaems in the active sites of the proteins.

#### Discussion

##### $\text{p}K_a$ values of the subunits of methHb A and methHb F

We first compared the  $\text{p}K_a$  values of the subunits of methHb A and methHb F in order to determine the non-equivalence in the haem environment among them. As shown in Table I, there is an appreciable difference in the  $\text{p}K_a$  value of the  $\alpha$  subunit between methHb A and methHb F. This finding indicated that the structural properties of the haem active site in the  $\alpha$

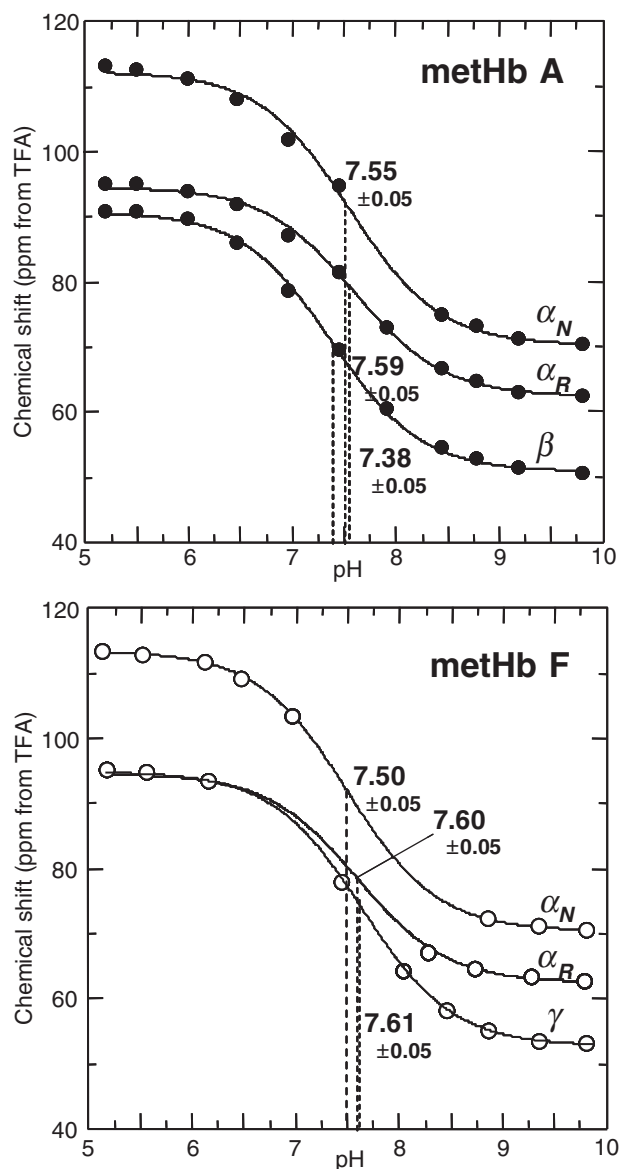


**Fig. 7** Plots of the shifts of the  $^{19}\text{F}$  NMR signals of methHb A(7-PF) (top) and methHb F(7-PF) (bottom) at  $25^\circ\text{C}$  as a function of pH.  $pK_a$  values of  $7.55 \pm 0.05$ ,  $7.59 \pm 0.05$  and  $7.38 \pm 0.05$  were obtained for the *N* and *R* forms of the  $\alpha$  subunit, and the  $\beta$  subunit of methHb A(7-PF), respectively; and those of  $7.50 \pm 0.05$ ,  $7.60 \pm 0.05$  and  $7.61 \pm 0.05$  for the *N* and *R* Forms of the  $\alpha$  subunit, and the  $\gamma$  subunit of methHb F(7-PF), respectively.

subunit are influenced by interactions between the constituent subunits of the protein ('inter-subunit interactions'). The  $pK_a$  value is affected by haem environment and the electronic nature of the haem peripheral side chains. Ferrihaem in methHb carries a net positive-charge, and hence needs to be stabilized by neutralization through electrostatic interaction with near-by polar groups in a hydrophobic haem environment. Consequently, as far as the stability of the ferrihaem in the protein is concerned, the alkaline form is more stable than the acidic one because of neutralization of the cationic character of ferrihaem by the coordinated  $\text{OH}^-$  (Scheme 1). On the other hand, as shown in Fig. 3, the Mulliken charge is affected by the  $\Psi_{3\text{-vinyl}}$  and  $\Psi_{8\text{-vinyl}}$  values. Since a decrease in the Mulliken charge is thought to represent an increase in the  $\rho_{\text{Fe}}$  value, the plots in Fig. 3 demonstrated that the  $\rho_{\text{Fe}}$  value increases with increasing the  $\Psi_{3\text{-vinyl}}$  and/or  $\Psi_{8\text{-vinyl}}$  values. The  $pK_a$  value has been shown to be closely related to the  $\rho_{\text{Fe}}$  value (33). The backward reaction of the acid–alkaline transition (Scheme 1) can be considered as protonation of the Fe-bound  $\text{OH}^-$ . Since a decrease in the  $\rho_{\text{Fe}}$  value results in removal of an electron from the Fe-bound  $\text{OH}^-$ , the proton affinity of the Fe-bound  $\text{OH}^-$  is thought to decrease with decreasing the  $\rho_{\text{Fe}}$  value, leading to a decrease in the  $pK_a$  value. Hence the  $pK_a$  value decreases with decreasing the  $\Psi_{3\text{-vinyl}}$  and/or  $\Psi_{8\text{-vinyl}}$  values.

X-ray structure of Hb F is available only for deoxy form, and X-ray structural comparison between the  $\alpha$  subunits of deoxy Hb A and Hb F indicated that there are sizable differences in the  $\Psi_{3\text{-vinyl}}$  and  $\Psi_{8\text{-vinyl}}$  values between them (Table IV) (3, 46, 49, 60), although their protein structures are highly alike (61, 46). Assuming that the larger  $\Psi_{3\text{-vinyl}}$  and  $\Psi_{8\text{-vinyl}}$  values for the  $\alpha$  subunit of Hb F relative to the corresponding values of Hb A, as observed in the X-ray structures of their deoxy forms, are retained in their met-forms, the  $pK_a$  value of the  $\alpha$  subunit of methHb F is expected to be higher than that of methHb A. Thus the higher  $pK_a$  value of the  $\alpha$  subunit of methHb F than that of methHb A could be attributed to the differences in the  $\Psi_{3\text{-vinyl}}$  and  $\Psi_{8\text{-vinyl}}$  values between the  $\alpha$  subunits of the two methHbs.

On the other hand, the difference in the  $pK_a$  value between the subunits of methHb A could be

**Table III.** The  $pK_a$  values of individual subunits of native methHb A, methHb F and the proteins reconstituted with meso and 7-PF at  $25^\circ\text{C}$ .

	methHb A				methHb F			
	proto <sup>a</sup>	meso	7-PF		proto <sup>a</sup>	meso	7-PF	
			<i>N</i> <sup>b</sup>	<i>R</i> <sup>b</sup>			<i>N</i> <sup>b</sup>	<i>R</i> <sup>b</sup>
$\alpha$	$8.32 \pm 0.05$	$8.52 \pm 0.05$	$7.55 \pm 0.05$	$7.59 \pm 0.05$	$8.48 \pm 0.05$	$8.50 \pm 0.05$	$7.50 \pm 0.05$	$7.60 \pm 0.05$
$\beta$	$7.48 \pm 0.05$	$8.52 \pm 0.05$	$7.38 \pm 0.05^c$		—	—	—	—
$\gamma$	—	—	—	—	$7.76 \pm 0.05$	$8.50 \pm 0.05$	$7.61 \pm 0.05^c$	

<sup>a</sup>Taken from native proteins. <sup>b</sup>*N* and *R* represent the normal and reversed haem orientations, respectively (Fig. 1B). <sup>c</sup>This subunit predominantly possesses a single heme orientation and the determination of the haem orientation could not be made from the present study (see text).



Table IV.  $\Psi_{3\text{-vinyl}}$  and  $\Psi_{8\text{-vinyl}}$  values of Hbs and isolated subunits.

Protein	$ \Psi_{3\text{-vinyl}} ^a$ (degree)			$ \Psi_{8\text{-vinyl}} ^a$ (degree)		
	$\alpha$	$\beta$	$\gamma$	$\alpha$	$\beta$	$\gamma$
Deoxy form						
Hb A <sup>b</sup>	33.2	32.0	—	31.0	32.8	—
	36.5	32.8	—	37.5	33.1	—
Hb F <sup>c</sup>	69.2	—	81.4	81.5	—	15.7
CO form						
Hb A <sup>b</sup>	32.7	6.0	—	38.3	23.9	—
		30.5	—		26.8	—
$\beta$ subunit <sup>d</sup>	—	48.2	—	—	30.8	—
		61.4	—		31.3	—
		71.6	—		31.6	—
$\gamma$ subunit <sup>c</sup>	—	—	49.3	—	—	39.6
			50.8			60.2

<sup>a</sup>The  $\Psi_{3\text{-vinyl}}$  and  $\Psi_{8\text{-vinyl}}$  values are indicated in the absolute values. In addition, since the orientation of the vinyl side chain  $\pi$  system with respect to the porphyrin  $\pi$  one is considered in the study, the values are indicated in the range of 0°–90°. Multiple entry represents disorder in the conformation of the vinyl side chains.

<sup>b</sup>Obtained from ref. 3. <sup>c</sup>Obtained from ref. 46. <sup>d</sup>Obtained from ref. 49. <sup>e</sup>Obtained from ref. 60.

interpreted in terms of their haem environments, because the  $\Psi_{3\text{-vinyl}}$  and  $\Psi_{8\text{-vinyl}}$  values of the  $\alpha$  and  $\beta$  subunits of metHb A are almost identical to each other (Table IV). In the case of metHb A, the  $pK_a$  value of the  $\alpha$  subunit is higher by  $\sim 0.8$  pH units than that of the  $\beta$  subunit. This finding could be attributed to a more polar haem environment in the  $\alpha$  subunit than the latter. This interpretation is supported from the study of autoxidation of oxy Hb A. Yasuda *et al.* (62) revealed that the autoxidation rate for the  $\alpha$  subunit is larger than that for the  $\beta$  one. The autoxidation rate is expected to increase with increasing polarity of the haem pocket. Therefore, the higher polarity of the haem environment in the  $\alpha$  subunit than that in the  $\beta$  one, as manifested in the larger autoxidation rate, is consistent with our interpretation, although the haem Fe oxidation and ligation states of the two systems are different from each other. Finally, considering the amino acid sequence homology between the  $\beta$  and  $\gamma$  subunits (see Supplementary Material SM1), the higher  $pK_a$  value for the  $\alpha$  subunit than the  $\gamma$  one in metHb F might also be attributed to a more polar haem environment in the former than the latter (see below).

#### Effects of hetero-tetramer assembly on the $pK_a$ values of the subunits

We next compared the  $pK_a$  values of the isolated subunits and metHbs in order to elucidate the effect of the hetero-tetramer assembly on the haem environments in the individual subunits. As indicated in Table I, the  $pK_a$  values of the isolated  $\alpha$ ,  $\beta$  and  $\gamma$  subunits were different from each other. Interestingly, the value of the isolated  $\gamma$  subunit was closer to that of the isolated  $\alpha$  subunit than that of the isolated  $\beta$  subunit, although the  $\beta$  and  $\gamma$  subunits exhibit high sequence homology of 73% (51). This finding clearly indicated that the  $pK_a$  value is determined solely by the haem local environment. The difference in the  $pK_a$  values between the

isolated  $\beta$  and  $\gamma$  subunits may be interpreted in terms of amino acid substitutions in them (Supplementary Material SM1). Among the 39 amino acid residue substitutions in the two subunits, two replacement sites, *i.e.* E14 and E15, are located in close proximity to the haem, and Ala E14 and Phe E15 in the  $\beta$  subunit are replaced by Ser and Leu in the  $\gamma$  subunit, respectively. Although E14 and E15 residues are located at least  $\sim 0.8$  nm away from haem iron, the replacements of the amino acid residues at these sites have been shown to alter the haem chemical environment largely enough to be manifested in the shifts of haem methyl proton NMR signals (63). Therefore, with these replacements, the polarity of the haem active site in the  $\gamma$  subunit is assumed to be higher than that in the  $\beta$  one, and hence the  $pK_a$  value of the former is expected to be higher than that of the latter. The  $pK_a$  value of the  $\gamma$  subunit was indeed larger than that of the  $\beta$  one (Table I). Furthermore, the  $\lambda_{\text{max}}$  value of Soret absorption of the isolated  $\gamma$  subunit was larger than that of the isolated  $\beta$  one (Table II), also supporting that the polarity of the haem environment in the  $\gamma$  subunit is higher than that in the  $\beta$  one, because the Soret absorption has been shown to exhibit bathochromic shift with increasing the polarity of solvent (59). In addition, the increase and decrease in the polarity of the haem environments of the  $\alpha$  subunit, and the  $\beta$  and  $\gamma$  subunits, respectively, upon the hetero-tetramer assembly, as suggested from the analysis of the  $\lambda_{\text{max}}$  values (Table II), are consistent with the observation that, for the  $\alpha$  subunit, the  $pK_a$  value of the isolated state is smaller than that of the Hb state, while, for the  $\beta$  and  $\gamma$  subunits, the values of the isolated states were larger than those of the Hb states (Table I).

The  $pK_a$  values of the  $\alpha$  subunits in metHb A and metHb F were higher by 0.15 and 0.31 pH unit, respectively, relative to that of the isolated  $\alpha$  subunit. On the other hand, the values of the  $\beta$  and  $\gamma$  subunits in metHb A and metHb F, respectively, were lower by 0.27 and 0.50 pH units, respectively, relative to those of the corresponding isolated subunits. As a result, the difference in the  $pK_a$  values between the  $\alpha$  and  $\beta$  subunits of metHb A [ $\Delta pK_a(\alpha/\beta)$ ], and similarly the difference in the  $pK_a$  values between the  $\alpha$  and  $\gamma$  subunits of metHb F [ $\Delta pK_a(\alpha/\gamma)$ ] is larger than that between the isolated  $\alpha$  and  $\beta$  subunits [ $\Delta pK_a(\alpha/\beta)$ ], and similarly the difference in the  $pK_a$  values between the  $\alpha$  and  $\gamma$  subunits of metHb F [ $\Delta pK_a(\alpha/\gamma)$ ] is larger than that between the isolated  $\alpha$  and  $\gamma$  subunits [ $\Delta pK_a(\alpha/\gamma)$ ]. Thus, the non-equivalence in the  $pK_a$  value between the constituent subunits, and hence the difference in the haem local environment between them, was found to be enhanced by the hetero-tetramer assembly. Such an asymmetric nature of active sites might be essential for allosteric proteins composed of multiple subunits.

#### Effects of hetero-tetramer assembly on the $pK_a$ values of the constituent subunits of valency hybrid Hbs

The effect of the hetero-tetramer assembly on the haem local environment was also reflected in the  $pK_a$  values of valency hybrid proteins. For all the subunits, the valency hybrid proteins exhibited a  $pK_a$  value between those of the corresponding subunits in the isolated and

tetrameric Hb states, *i.e.* for the  $\alpha$  subunits of both metHb A and metHb F, the  $pK_a$  value of the valency hybrid state is larger and smaller than those of the isolated and Hb states, respectively, and, on the other hand, for the  $\beta$  and  $\gamma$  subunits of metHb A and metHb F, the value of the valency hybrid state is smaller and larger than those of the isolated and Hb states, respectively. These results demonstrated that the  $pK_a$  value of a subunit is affected by not only the hetero-tetramer assembly, but also the haem Fe oxidation and ligation states of the partner subunit.

The subunit interactions in Hb A and Hb F enable communication between the haem active sites of the constituent subunits of the proteins. Hence the molecular mechanisms responsible for the subunit interactions in the protein are likely to involve structural changes in not only the sites of inter-subunits interaction, but also the contact between haem and the protein at the active site ('haem–protein interactions'). As described above, the effect of the hetero-tetramer assembly on the haem environment was clearly manifested in the  $pK_a$  values of the subunits. Furthermore, the effect of the haem–protein interactions on the inter-subunit interaction was also manifested in the differences in the  $pK_a$  values of the subunits between the valency hybrid and Hb states. These results confirmed the presence of a pathway for transmission of a structural change of one subunit to the other ones within tetrameric Hb, although its molecular mechanism is remained to be elucidated.

#### **Haem active site structures of metHb A(7-PF) and metHb F(7-PF)**

Because of its wide spectral range,  $^{19}\text{F}$  NMR is remarkably sensitive as to the local magnetic environment, exhibiting not only extremely high resolution of signals, but also a large dynamic range (41). Well-resolved signals were observed in the  $^{19}\text{F}$  NMR spectra of metHb A(7-PF) and metHb F(7-PF) (Fig. 6A). The shift differences between the signals due to the haem orientational disorder in the  $\alpha$  subunits of metHb A(7-PF) and metHb F(7-PF) are similar to each other, and are larger than that in the case of metMb(7-PF). The shifts of the signals have been shown to sharply reflect the unpaired electron delocalization of the haem, which is predominantly determined by the nature of the axial ligands (64, 65). Consequently, the present results suggested that the  $\Phi$  angle between the projection of the axial His imidazole onto the haem plane and the  $\text{N}_{\text{II}}\text{-Fe-N}_{\text{IV}}$  axis (Fig. 1B) of the  $\alpha$  subunits of metHb A(7-PF) and metHb F(7-PF) are similar to each other, and are smaller than that in the case of metMb(7-PF), although the X-ray crystal structures of the native proteins indicated that the  $\Phi$  angles of the  $\alpha$  subunits of native Hb A and Hb F, and met Mb are similar to each other (3, 47).

#### **Haem Orientational Disorder in metHb A(7-PF) and metHb F(7-PF)**

Analysis of the signal intensities in  $^{19}\text{F}$  NMR spectra revealed that the *N* form: *R* form ratios for the  $\alpha$  subunits of metHb A(7-PF) and metHb F(7-PF) are  $\sim 1:3$ ,

and essentially no haem orientational disorder was detected in the  $\beta$  and  $\gamma$  subunits of either protein. These ratios were different from that for metMb(7-PF), *i.e.* *N* form: *R* form = 1.0:2.2 (31). Considering the symmetry of the 7-PF molecular structure, it is obvious that steric contact between the haem peripheral side chains attached at positions 2, 3, 7 and 8, and near-by amino acid residues is crucial for the thermodynamic stabilities of the *N* and *R* forms. The haem side chains at positions 2, 3, 7 and 8 are in close contact with the amino acid residues at E10:E14:F4, E15:G5:G8:G12:H15, B13:FG5:G4:G8 and B13:CD1:C4:C7:FG5:G4, respectively (3, 46). Among these residues, amino acid replacements were found at the B13 and C7 positions between the  $\alpha$  and  $\beta$  (or  $\gamma$ ) subunits, *i.e.* Met B13 and Tyr C7 in the  $\alpha$  subunit are replaced by Leu and Phe in the  $\beta$  (or  $\gamma$ ) subunit, respectively (Supplementary Material SM1) (3, 46). Furthermore, in the case of Mb, Leu and Lys occupy B13 and C7, respectively (see Supplementary Material SM1) (2). Consequently, the amino acid residue at C7 may play a role in determination of the thermodynamics of the haem orientational disorder of 7-PF in the subunits of Hbs and Mb. According to the X-ray crystal structures of native Hb A and Mb (3, 66), the side chains of Tyr C7 and Lys C7 in the  $\alpha$  subunit and Mb, respectively, point somewhat away from the haem, and are hydrogen bonded to the side chain  $\text{NH}_2$  group of Asn G4 and carbonyl oxygen of Lys FG4, respectively. Hence the contact between the haem side chain at position 8 and the C7 residue in the  $\alpha$  subunit and Mb would not be so tight. On the other hand, the side chain of Phe C7 of the  $\beta$  subunit is in close contact with haem, leading to tight contact with the haem side chain at position 8. Such steric hindrance might render the energy difference between the two haem orientations, *i.e.* the *N* and *R* forms, large enough to almost completely inhibit one of the orientations.

#### **$pK_a$ values of reconstituted metHbs**

We finally analysed the effect of the haem substitution on the  $pK_a$  values of the subunits of metHbs in order to determine the effect of alteration of the haem–protein interaction on the haem environments of the proteins. In the case of the metHb A system, both the  $\alpha$  and  $\beta$  subunits of metHb A(Meso) exhibited  $pK_a$  values of  $\sim 8.5$ , and values of  $7.55 \pm 0.05$ ,  $7.59 \pm 0.05$  and  $7.38 \pm 0.05$  were obtained for the *N* and *R* forms of the  $\alpha$  subunit, and the  $\beta$  subunit of metHb A(7-PF), respectively (Table I). Since mesohaem and 7-PF differ from each other only in the substituent at position 7 (Fig. 1A), the decrease in the  $pK_a$  value by  $\sim 1$  pH unit upon the haem replacement from the former to the latter demonstrated the significant effect of the  $\text{CF}_3$  substitution on the acid–alkaline transition. The substitution of the electron-withdrawing  $\text{CF}_3$  group for the haem peripheral  $\text{CH}_3$  side chain decreases the  $\rho_{\text{Fe}}$  value, leading to a decrease in the  $pK_a$  value (33).

The haem substitution also influenced the non-equivalence of the  $pK_a$  values of the constituent subunits of Hbs. In the case of metHb A, the  $\Delta pK_a(\text{A})$  value was significantly decreased by the haem substitution, *i.e.* the  $\Delta pK_a(\text{A})$  values were  $\sim 0.8$ , 0 and 0.2

pH unit for metHb A, metHb A(Meso) and metHb A(7-PF), respectively (Table III). Similarly, since the values of  $7.50 \pm 0.05$ ,  $7.60 \pm 0.05$  and  $7.61 \pm 0.05$  were obtained for the *N* and *R* forms of the  $\alpha$  subunit, and the  $\gamma$  subunit of metHb F(7-PF), respectively (Table III), the  $\Delta pK_a(F)$  value was also decreased by the haem substitution, *i.e.* the  $\Delta pK_a(F)$  values were  $\sim 0.7$  and 0 pH units for metHb F and metHb F(7-PF), respectively. Thus, the substitution of the native haem, *i.e.* protohaem, by mesohaem or 7-PF was found to reduce the non-equivalence of the haem environment of the constituent subunits of the proteins. As described earlier, since the  $pK_a$  values of the subunits of the proteins have been shown to be affected by the inter-subunit interactions and the haem–protein interaction, the decrease in the  $\Delta pK_a(A)$  [or  $\Delta pK_a(F)$ ] value on the haem replacement could be due to alteration of the haem–protein interaction. The substitution of the haem peripheral vinyl side chains by ethyl groups, as a result of the haem replacement from protohaem to mesohaem (or 7-PF), should significantly alter the haem–protein interaction. Furthermore, the cooperative ligand binding of Hb A has been shown to be affected by the haem–protein interaction, especially the contacts between the haem peripheral side chains attached to pyrroles I and II, and the protein (67). Consequently, the present results demonstrated that the interaction between the haem vinyl side chain and protein contributes significantly to maintain not only the non-equivalence of the haem active sites of the constituent subunits of the proteins, but also the inter-subunit interaction essential for the cooperative oxygen binding of the protein. In fact, the oxygen binding study on Hb A demonstrated that the cooperativity, as measured as Hill's *n*-value, decreased from 3.2 to 1.6 with the replacement of protohaem by mesohaem (68), indicating the importance of the haem vinyl groups for the subunit interaction.

## Supplementary Data

Supplementary Data are available at *JB* Online.

## Acknowledgements

The  $^{19}\text{F}$  NMR spectra were recorded on a Bruker AVANCE-500 spectrometer at the Chemical Analysis Center, University of Tsukuba.

## Funding

Grant-in-aid for Scientific Research on Innovative Areas (No. 21108505, ' $\pi$ -Space') from the Ministry of Education, Culture, Sports, Science and Technology, Japan; the Yazaki Memorial Foundation for Science and Technology, and the NOVARTIS Foundation (Japan) for the Promotion of Science.

## Conflict of interest

None declared.

## References

- Perutz, M.F., Wilkinson, A.J., Paoli, M., and Dodson, G.G. (1998) The stereochemical mechanism of the cooperative effects in hemoglobin revisited. *Annu. Rev. Biophys. Biomol. Struct.* **27**, 1–34
- Dickerson, R.E. and Geis, I. (1983) *Hemoglobin: Structure, Function, Evolution, and Pathology*, Benjamin/Cummings, Menlo Park, CA
- Park, S.Y., Yokoyama, T., Shibayama, N., Shiro, Y., and Tame, J.R.H. (2006) 1.25 Å resolution crystal structures of human haemoglobin in the oxy, deoxy and carbonmonoxy forms. *J. Mol. Biol.* **360**, 690–701
- Imai, K. (1981) Measurement of accurate oxygen equilibrium curves by an automatic oxygenation apparatus *Methods in Enzymology* (Antonini, E., Rossi-Bernardi, L., and Chiancone, E., eds.) Vol. 76, pp. 438–449, Academic Press, New York
- Antonini, E. and Brunori, M. (1971) *Hemoglobins and Myoglobins in their Reactions with Ligands*. Chapters 2 and 3, North Holland Publishing, Amsterdam
- Blough, N.V., Zemel, H., Hoffman, B.M., Lee, T.C.K., and Gibson, Q.H. (1980) Kinetics of CO binding to manganese, zinc, and cobalt hybrid hemoglobins. *J. Am. Chem. Soc.* **102**, 5683–5685
- Inubushi, T., Ikeda-Saito, M., and Yonetani, T. (1983) Isotropically shifted NMR resonances for the proximal histidyl imidazole NH protons in cobalt hemoglobin and iron-cobalt hybrid hemoglobins. Binding of the proximal histidine toward porphyrin metal ion in the intermediate state of cooperative ligand binding. *Biochemistry* **22**, 2904–2907
- Blough, N.V. and Hoffman, B.M. (1984) Carbon monoxide binding to the ferrous chains of [Mn, Fe(II)] hybrid hemoglobins: pH dependence of the chain affinity constants associated with specific hemoglobin ligation pathways. *Biochemistry* **23**, 2875–2882
- Shibayama, N., Morimoto, H., and Miyazaki, G. (1986) Oxygen equilibrium study and light absorption spectra of Ni(II)-Fe(II) hybrid hemoglobins. *J. Mol. Biol.* **192**, 323–329
- Inubushi, T., D'Ambrosio, C., Ikeda-Saito, M., and Yonetani, T. (1986) NMR studies of monoligated Fe-Co hybrid hemoglobins: their quaternary structure and proximal histidine coordination. *J. Am. Chem. Soc.* **108**, 3799–3803
- Shibayama, N., Ikeda-Saito, M., Hori, H., Itaroku, K., Morimoto, H., and Saigo, S. (1995) Oxygen equilibrium and electron paramagnetic resonance studies on copper(II)-iron(II) hybrid hemoglobins at room temperature. *FEBS Lett.* **372**, 126–130
- Bowen, J.H., Shokhirev, N.V., Raitsimring, A.M., Buttlare, D.H., and Walker, F.A. (1997) EPR studies of the dynamics of rotation of dioxygen in model cobalt(II) hemes and cobalt-containing hybrid hemoglobins. *J. Phys. Chem. B* **101**, 8683–8691
- Unzai, S., Eich, R., Shibayama, N., Olson, J.S., and Morimoto, H. (1998) Rate constants for O<sub>2</sub> and CO binding to the  $\alpha$  and  $\beta$  subunits within the R and T states of human hemoglobin. *J. Biol. Chem.* **273**, 23150–23159
- Miyazaki, G., Morimoto, H., Yun, K.-M., Park, S.-Y., Nakagawa, A., Minagawa, H., and Shibayama, M. (1999) Magnesium(II) and zinc(II)-protoporphyrin IX's stabilize the lowest oxygen affinity state of human hemoglobin even more strongly than deoxyheme. *J. Mol. Biol.* **292**, 1121–1136
- Nagatomo, S., Nagai, M., Shibayama, N., and Kitagawa, T. (2002) Differences in changes of the  $\alpha 1$ - $\beta 2$  subunit contacts between ligand binding to the  $\alpha$  and  $\beta$  subunits of hemoglobin A: UV resonance Raman analysis using Ni-Fe hybrid hemoglobin. *Biochemistry* **41**, 10010–10020

16. Samuni, U., Juszczak, L., Dantsker, D., Khan, I., Friedman, A.J., Pérez-González-de-Apodaca, J., Bruno, S., Hui, H.L., Colby, J.E., Karasik, E., Kwiatkowski, L.D., Mozzarelli, A., Noble, R., and Friedman, J.M. (2003) Functional and spectroscopic characterization of half-liganded iron–zinc hybrid hemoglobin: evidence for conformational plasticity within the T state. *Biochemistry* **42**, 8272–8288
17. Simplaceanu, V., Lukin, J.A., Fang, T.-Y., Zou, M., Ho, N.T., and Ho, C. (2000) Chain-selective isotopic labeling for NMR studies of large multimeric proteins: application to hemoglobin. *Biophys. J.* **79**, 1146–1154
18. Song, X.-J., Simplaceanu, V., Lukin, J.A., Ho, N.T., and Ho, C. (2008) Effector-induced structural fluctuation regulates the ligand affinity of an allosteric protein: binding of inositol hexaphosphate has distinct dynamic consequences for the T and R states of hemoglobin. *Biochemistry* **47**, 4907–4915
19. Hu, X. and Spiro, T.G. (1997) Tyrosine and tryptophan structure markers in hemoglobin ultraviolet resonance Raman spectra: mode assignments via subunit-specific isotope labeling of recombinant protein. *Biochemistry* **36**, 15701–15712
20. Balakrishnan, G., Zhao, X., Podstawska, E., Proniewicz, L.M., Kincaid, J.R., and Spiro, T.G. (2009) Subunit-selective interrogation of CO recombination in carbon-monooxygenase hemoglobin by isotope-edited time-resolved resonance Raman spectroscopy. *Biochemistry* **48**, 3120–3126
21. Nagai, K. and Kitagawa, T. (1980) Differences in Fe(II)-N<sub>6</sub>(His-F8) stretching frequencies between deoxyhemoglobins in the two alternative quaternary structures. *Proc. Natl Acad. Sci. USA* **77**, 2033–2037
22. Jue, T., La Mar, G.N., Han, K.-H., and Yamamoto, Y. (1984) NMR study of the exchange rates of allosterically responsive labile protons in the heme pockets of hemoglobin A. *Biophys. J.* **46**, 117–120
23. Han, K.-H. and La Mar, G.N. (1986) Nuclear magnetic resonance study of the isotope exchange of the proximal histidyl ring labile protons in hemoglobin A: the exchange rates and mechanisms of individual subunits in deoxy and oxy-hemoglobin. *J. Mol. Biol.* **189**, 541–552
24. Giacometti, G.M., Da Ros, A., Antonini, E., and Brunori, M. (1975) Equilibrium and kinetics of the reaction of Aplysia myoglobin with azide. *Biochemistry* **14**, 1584–1588
25. Iizuka, T. and Morishima, I. (1975) NMR studies of hemoproteins. VI. Acid-base transitions of ferric myoglobin and its imidazole complex. *Biochim. Biophys. Acta* **400**, 143–153
26. McGrath, T.M. and La Mar, G.N. (1978) Proton NMR study of the thermodynamics and kinetics of the acid in equilibrium base transitions in reconstituted metmyoglobins. *Biochim. Biophys. Acta* **534**, 99–111
27. Pande, U., La Mar, G.N., Lecomte, J.T.L., Ascoli, F., Brunori, M., Smith, K.M., Pandey, R.K., Parish, D.W., and Thanabal, V. (1986) NMR study of the molecular and electronic structure of the heme cavity of Aplysia metmyoglobin. Resonance assignments based on isotope labeling and proton nuclear Overhauser effect measurements. *Biochemistry* **25**, 5638–5646
28. Yamamoto, Y., Osawa, A., Inoue, Y., Chûjô, R., and Suzuki, T. (1990) A <sup>1</sup>H-NMR study of electronic structure of the active site of Galeorhinus japonicus metmyoglobin. *Eur. J. Biochem.* **192**, 225–229
29. Yamamoto, Y., Chûjô, R., Inoue, Y., and Suzuki, T. (1992) Kinetic characterization of the acid-alkaline transition in Dolabella auricularia ferric myoglobin using <sup>1</sup>H-NMR saturation transfer experiments. *FEBS Lett.* **310**, 71–74
30. Yamamoto, Y., Suzuki, T., and Hori, H. (1993) Dynamics and thermodynamics of acid-alkaline transitions in metmyoglobins lacking the usual distal histidine residue. *Biochim. Biophys. Acta* **1203**, 267–275
31. Nagao, S., Hirai, Y., Suzuki, A., and Yamamoto, Y. (2005) <sup>19</sup>F NMR characterization of the thermodynamics and dynamics of the acid-alkaline transition in a reconstituted sperm whale metmyoglobin. *J. Am. Chem. Soc.* **127**, 4146–4147
32. Shu, F., Ramakrishnan, V., and Schoenborn, B.P. (2000) Enhanced visibility of hydrogen atoms by neutron crystallography on fully deuterated myoglobin. *Proc. Natl Acad. Sci. USA* **97**, 3872–3877
33. Shibata, T., Nagao, S., Fukaya, M., Tai, H., Nagatomo, S., Morihashi, K., Matsuo, T., Hirota, S., Suzuki, A., Imai, K., and Yamamoto, Y. (2010) Effect of heme modification on oxygen affinity of myoglobin and equilibrium of the acid-alkaline transition in metmyoglobin. *J. Am. Chem. Soc.* **132**, 6091–6098
34. La Mar, G.N., Budd, D.L., Viscio, D.B., Smith, K.M., and Langry, L.C. (1978) Proton nuclear magnetic resonance characterization of heme disorder in hemoproteins. *Proc. Natl Acad. Sci. USA* **75**, 5755–5759
35. Cassoly, R. (1981) Preparation of hemoglobin hybrid carrying different ligands: valency hybrids and related compounds. *Methods in Enzymology* (Antonini, E., Rossi-Bernardi, L., and Chiancone, E., eds.) Vol. 76, pp. 106–113, Academic Press, New York
36. Toi, H., Homma, M., Suzuki, A., and Ogoshi, H. (1985) Paramagnetic <sup>19</sup>F n.m.r. spectra of iron(III) porphyrins substituted with CF<sub>3</sub> groups and reconstituted myoglobin. *J. Chem. Soc. Chem. Commun.* 1791–1792
37. Yamamoto, Y., Hirai, Y., and Suzuki, A. (2000) <sup>19</sup>F NMR study of protein-induced rhombic perturbations on the electronic structure of the active site of myoglobin. *J. Biol. Inorg. Chem.* **5**, 455–462
38. Hirai, Y., Yamamoto, Y., and Suzuki, A. (2000) <sup>19</sup>F NMR study of the heme orientation and electronic structure in a myoglobin reconstituted with a ring-fluorinated heme. *Bull. Chem. Soc. Jpn.* **73**, 2309–2316
39. Yamamoto, Y., Nagao, S., Hirai, Y., Inose, T., Terui, N., Mita, H., and Suzuki, A. (2004) NMR investigation of the heme electronic structure in deoxymyoglobin possessing a fluorinated heme. *J. Biol. Inorg. Chem.* **9**, 152–160
40. Hirai, Y., Nagao, S., Mita, H., Suzuki, A., and Yamamoto, Y. (2004) <sup>19</sup>F NMR study on the heme electronic structure in oxy and carbonmonoxy reconstituted myoglobins. *Bull. Chem. Soc. Jpn.* **77**, 1485–1486
41. Yamamoto, Y. (1998) NMR study of active sites in paramagnetic hemoproteins. *Annu. Rep. NMR Spectrosc.* **36**, 1–77
42. Hull, W.E. and Sykes, B.D. (1974) Fluorotyrosine alkaline phosphatase. <sup>19</sup>F nuclear magnetic resonance relaxation times and molecular motion of the individual fluorotyrosines. *Biochemistry* **13**, 3431–3437
43. Hull, W.E. and Sykes, B.D. (1975) Fluorotyrosine alkaline phosphatase: internal mobility of individual tyrosines and the role of chemical shift anisotropy as a <sup>19</sup>F nuclear spin relaxation mechanism in proteins. *J. Mol. Biol.* **98**, 121–153
44. Gueron, M. (1975) Nuclear relaxation in macromolecules by paramagnetic ions. Novel mechanism. *J. Magn. Reson.* **19**, 58–66
45. Vega, A.J. and Fiat, D. (1976) Nuclear relaxation processes of paramagnetic complexes. The slow-motion case. *Mol. Phys.* **31**, 347–355

46. Frier, J.A. and Perutz, M.F. (1977) Structure of human foetal deoxyhaemoglobin. *J. Mol. Biol.* **112**, 97–112
47. Valdes, R. Jr and Ackers, G.K. (1977) Thermodynamic studies on subunit assembly in human hemoglobin. Self-association of oxygenated chains (alphaSH and betaSH): determination of stoichiometries and equilibrium constants as a function of temperature. *J. Biol. Chem.* **252**, 74–81
48. Borgstahl, G.E.O., Rogers, P.H., and Arnone, A. (1994) The 1.9 Å structure of deoxy beta 4 hemoglobin. Analysis of the partitioning of quaternary-associated and ligand-induced changes in tertiary structure. *J. Mol. Biol.* **236**, 831–843
49. Borgstahl, G.E.O., Rogers, P.H., and Arnone, A. (1994) The 1.8 Å structure of carbonmonoxy-beta 4 hemoglobin. Analysis of a homotetramer with the R quaternary structure of liganded alpha 2 beta 2 hemoglobin. *J. Mol. Biol.* **236**, 817–830
50. La Mar, G.N., Yamamoto, Y., Jue, T., Smith, K.M., and Pandey, R.K. (1985) <sup>1</sup>H NMR characterization of metastable and equilibrium heme orientational heterogeneity in reconstituted and native human hemoglobin. *Biochemistry* **24**, 3826–3831
51. Prins, H.K. (1956) Separation of different types of human hemoglobin. *J. Chromatogr.* **2**, 445–486
52. Bucci, E. and Fronticelli, C. (1965) A new method for the preparation of alpha and beta subunits of human hemoglobin. *J. Biol. Chem.* **240**, 551–552
53. Noble, R.W. (1971) The effect of p-hydroxymercuribenzoate on the reactions of the isolated gamma chains of human hemoglobin with ligands. *J. Biol. Chem.* **246**, 2972–2976
54. Tomoda, A., Takeshita, M., and Yoneyama, Y. (1978) Characterization of intermediate hemoglobin produced during methemoglobin reduction by ascorbic acid. *J. Biol. Chem.* **253**, 7415–7419
55. Banerjee, R. and Cassoly, R. (1969) Oxygen equilibria of human hemoglobin valency hybrids. Discussion on the intrinsic properties of alpha and beta chains in the native protein. *J. Mol. Chem.* **42**, 351–361
56. Teale, F.W.J. (1959) Cleavage of the haem-protein link by acid methylethylketone. *Biochim. Biophys. Acta* **35**, 543
57. Frisch, M.J., Trucks, G.W., Schlegel, H.B., Scuseria, G.E., Robb, M.A., Cheeseman, J.R., Montgomery, J.A. Jr, Vreven, T., Kudin, K.N., Burant, J.C., Millam, J.M., Iyengar, S.S., Tomasi, J., Barone, V., Mennucci, B., Cossi, M., Scalmani, G., Rega, N., Petersson, G.A., Nakatsuji, H., Hada, M., Ehara, M., Toyota, K., Fukuda, R., Hasegawa, J., Ishida, M., Nakajima, T., Honda, Y., Kitao, O., Nakai, H., Klene, M., Li, X., Knox, J.E., Hratchian, H.P., Cross, J.B., Bakken, V., Adamo, C., Jaramillo, J., Gomperts, R., Stratmann, R.E., Yazyev, O., Austin, A.J., Cammi, R., Pomelli, C., Ochterski, J.W., Ayala, P.Y., Morokuma, K., Voth, G.A., Salvador, P., Dannenberg, J.J., Zakrzewski, V.G., Dapprich, S., Daniels, A.D., Strain, M.C., Farkas, O., Malick, D.K., Rabuck, A.D., Raghavachari, K., Foresman, J.B., Ortiz, J.V., Cui, Q., Baboul, A.G., Clifford, S., Cioslowski, J., Stefanov, B.B., Liu, G., Liashenko, A., Piskorz, P., Komaromi, I., Martin, R.L., Fox, D.J., Keith, T., Al-Laham, M.A., Peng, C.Y., Nanayakkara, A., Challacombe, M., Gill, P.M.W., Johnson, B., Chen, W., Wong, M.W., Gonzalez, C., and Pople, J.A. (2004) *Gaussian 03*, Revision E.01, Gaussian, Inc, Wallingford, CT
58. Banerjee, R., Alpert, Y., Letterier, F., and Williams, R.J.P. (1969) Visible absorption and electron spin resonance spectra of the isolated chains of human hemoglobin. Discussion of chain-mediated heme-heme interaction. *Biochemistry* **8**, 2862–2867
59. Falk, J.E. (1994) *Porphyrin and Metalloporphyrins*. Elsevier, Amsterdam
60. Kidd, R.D., Baker, H.M., Mathews, A.J., Brittain, T., and Baker, E.N. (2001) Oligomerization and ligand binding in a homotetrameric hemoglobin: two high-resolution crystal structures of hemoglobin Bart's (gamma(4)), a marker for alpha-thalassemia. *Protein Sci.* **10**, 1739–1749
61. Liddington, R., Derewenda, Z., Dodson, E., Hubbard, R., and Dodson, G. (1992) High resolution crystal structures and comparisons of T-state deoxyhaemoglobin and two liganded T-state haemoglobins: T(alpha-oxy)haemoglobin and T(met)haemoglobin. *J. Mol. Biol.* **228**, 551–579
62. Yasuda, J., Ichikawa, T., Tsuruga, M., Matsuoka, A., Sugawara, Y., and Shikama, K. (2002) The alpha 1 beta 1 contact of human hemoglobin plays a key role in stabilizing the bound dioxygen. *Eur. J. Biochem.* **269**, 202–211
63. Yamamoto, Y. and Nagaoka, T. (1998) A <sup>1</sup>H NMR comparative study of human adult and fetal hemoglobins. *FEBS Lett.* **424**, 169–172
64. Yamamoto, Y., Nanai, N., Chujo, R., and Suzuki, T. (1990) Heme methyl hyperfine shift pattern as a probe for determining the orientation of the functionally relevant proximal histidyl imidazole with respect to the heme in hemoproteins. *FEBS Lett.* **264**, 113–116
65. Shokhirev, N.V. and Walker, F.A. (1998) The effect of axial ligand plane orientation on the contact and pseudocontact shifts of low-spin ferriheme proteins. *J. Biol. Inorg. Chem.* **3**, 581–594
66. Vojtěchovský, J., Chu, K., Berendzen, J., Sweet, R.M., and Schlichting, I. (1999) Crystal structures of myoglobin-ligand complexes at near-atomic resolution. *Biophys. J.* **77**, 2153–2174
67. Nagai, M., Nagai, Y., Aki, Y., Imai, K., Wada, Y., Nagatomo, S., and Yamamoto, Y. (2008) Effect of reversed heme orientation on circular dichroism and cooperative oxygen binding of human adult hemoglobin. *Biochemistry* **47**, 517–525
68. Sugita, Y. and Yoneyama, Y. (1971) Oxygen equilibrium of hemoglobins containing unnatural hemes. Effect of modification of heme carboxyl groups and side chains at positions 2 and 4. *J. Biol. Chem.* **246**, 389–394